Anterior gradient protein 2 is a marker of tumor aggressiveness in breast cancer and favors chemotherapy-induced senescence escape

AMINE MAAROUF, ALICE BOISSARD, CÉCILE HENRY, GÉRALDINE LEMAN,
OLIVIER COQUERET, CATHERINE GUETTE and ERIC LELIÈVRE

Paul Papin ICO Cancer Center, CRCINA, INSERM U1232, Université de Nantes, Université d'Angers, 49055 Angers, France

Abstract. Among the different chemotherapies available, genotoxic drugs are widely used. In response to these drugs, particularly doxorubicin, tumor cells can enter into senescence. Chemotherapy-induced senescence (CIS) is a complex response. Long described as a definitive arrest of cell proliferation, the present authors and various groups have shown that this state may not be complete and could allow certain cells to reproliferate. The mechanism could be due to the activation of new signaling pathways. In the laboratory, the proteins involved in these pathways and triggering cell proliferation were studied. The present study determined a new role for anterior gradient protein 2 (AGR2) *in vivo* in patients and *in vitro* in a senescence escape model. AGR2's implication in breast cancer patients and proliferation of senescent cells was assessed based on a SWATH-MS proteomic study of patients' samples and RNA interference technology on cell lines. First, AGR2 was identified and it was found that its concentration is higher in the serum of patients with breast cancer and that this high concentration is associated with metastasis occurrence. An inverse correlation between intratumoral AGR2 expression and the senescence marker p16 was also observed. This observation led to the study of the role of AGR2 in the CIS escape model. In this model, it was found that AGR2 is overexpressed in cells during senescence escape and that its loss considerably reduces this phenomenon. Furthermore, it was shown that the extracellular form of AGR2 stimulated the reproliferation of senescent cells. The power of proteomic analysis based on the SWATH-MS approach allowed the present study to highlight the mammalian target of rapamycin (mTOR)/AKT signaling pathway in the senescence escape mechanism mediated by AGR2. Analysis of the two signaling pathways revealed that AGR2 modulated RICTOR and AKT phosphorylation. All these results showed that AGR2 expression in sera and tumors of breast cancer patients is a marker of tumor progression and metastasis occurrence. They also showed that its overexpression regulates CIS escape via activation of the mTOR/AKT signaling pathway.

Introduction

Senescence is a cellular stress response triggered by various stressors, including oncogene activation, telomere shortening and genotoxic treatments (1). The definitive arrest of proliferation in most cases is led by the p53/p21 and p16/Rb signaling pathways in response to DNA damage (2,3), which then induces irreversible proliferative arrest. Furthermore, senescent cells present specific hallmarks, such as DNA damage, that can be revealed by γH2Ax staining, the Senescence-Associated Secretory Phenotype, and a compaction of proliferative genes termed Senescence-Associated Heterochromatin Foci (4).

Senescence can be induced in response to chemotherapy (Chemotherapy-Induced Senescence; CIS) and was initially considered as a favorable outcome (5). The proliferative arrest observed during senescence has long been perceived as a definitive end to proliferation (1,6). However, several studies and experiments show that cells are able to overcome this state and proliferate again. The authors and other laboratories have demonstrated that chemotherapy-induced senescence is incomplete. As a result, some cells can proliferate and become more aggressive (1,7,8).

Proteomics is a powerful tool to search for markers in various pathological processes and particularly in oncology. The authors' laboratory uses a mass spectrometry approach to identify and study deregulated proteins, such as Olfactomedin 4 (OLFM4) and Thrombospondin 1 (TSP1), in tumor samples from patients (9,10). A proteome study identified Human Anterior Gradient protein 2 (AGR2), which is implicated in cancer development and metastasis induction, especially in breast cancer (9).

AGR2, a member of the human Protein Disulfide Isomerase family, is involved in protein folding in the endoplasmic reticulum (ER) (11,12). A number of studies have shown that AGR2, which is resident in the ER to regulate peptide maturation, can be secreted and act on the tumor niche in an

auto- and paracrine manner (13-16). These two forms of the protein seem to result from a state of equilibrium between the monomeric and dimeric forms regulating the activities of the molecule (17). Although it was originally described as a developmental protein (18), a number of studies have shown variation in its expression in different types of cancer cells (15,19-23). Its overexpression and pro-tumoral role were first shown in breast cancer and described in other tissues such as the esophagus, pancreas, lungs and ovaries (23).

In breast cancer tumors, AGR2 expression correlates with the expression of estrogen receptor (24). This receptor regulates AGR2 expression following stimulation by estradiol or tamoxifen (25). The overexpression of AGR2 in breast cancer tumors can be responsible for the induction of cell proliferation through the regulation of proliferative proteins such as cyclin D1, c-Myc and E2F1 (26). AGR2 expression is also associated with tumor aggressivity by inducing metastasis (27). Finally, it was observed that cells overexpressing AGR2 show treatment resistance toward tamoxifen and doxorubicin (28,29).

The author's laboratory studies the expression of various proteins in colorectal cancer and breast cancer to identify new biomarkers that allow tumor and metastasis detection. These proteomic studies are also combined with a CIS escape model to determine the pathways that lead to senescence escape.

The aim of the present study was to determine a role of the AGR2 protein *in vivo* and evaluate its potential role as a biomarker of prognosis in patients with breast cancer. It also determined its new role *in vitro*, specifically in a chemotherapy-induced senescence model and the impact of its intracellular and extracellular forms on the activation of proliferative pathways.

Material and methods

Cell lines and treatments. MCF-7 and LS174T cell lines were obtained from the American Type Culture Collection. Cell lines were authenticated by STR profiling and regularly tested to exclude mycoplasma contamination. To induce senescence, MCF-7 and LS174T cells were treated in RPMI medium (Dutscher; cat. no. L0500-500) containing 3% fetal bovine serum (FBS) (Eurobio; cat. no. CVFSVF00 01) respectively with doxorubicin (Tocris Bioscience; cat. no. 2252) (25 ng/ml) and sn38 (Tocris Bioscience; cat. no. 2684) (5 ng/ml) for 96 h. To promote senescence escape, cells were washed with PBS and stimulated with fresh medium containing 10% FBS for the indicated time. AKT inhibitor [iAKT1/2:1,3-Dihydro-1-(1-[(4-[6-phenyl-1H-imidazo(4,5-g)quinoxalin-7-yl]phenyl)methyl]-4-piperidinyl)-2H-benzimidazol-2-one trifluoroacetate; Sigma-Aldrich; Merck KGaA; cat. no. A6730] was used at a concentration of 100 μM and Torin (Cell Signaling Technology, Inc.; cat. no. 14379) at 10 nM.

Emerging cells. MCF-7 and LS174T cells were treated in RPMI medium containing 3% FBS respectively with doxorubicin (25 ng/ml) and sn38 (5 ng/ml) for 96 h. To obtain an emerging population, comprising proliferative and senescent cells, senescent cells were washed with PBS and fresh media was added for 7 or 11 days.

Small interfering (si)RNA transfection. Cells were transfected with 50 nM of siRNA directed against AGR2 (5'-CUG

AUUAGGUUAUGGUUUATT-3') (30) and prevalidated control siRNA (Dharmacon; cat. no. D-001810-10-20) using DharmaFECT-4 (Dharmacon). The cells were incubated for 24 h at 37°C, then the media was changed into fresh RPMI 10% FBS for an extra 24 h for western blot experiments or 9 days for emergence experiments.

Extracellular (e)AGR2
Plasmid transfection and conditioned media generation. For transfection experiments, MCF-7 and 293 cells were seeded into 10 cm culture dishes and grown until 80% confluence. Then, 2.5 μg of the empty vector pcDNA3.0 and the pcDNA3.0/AGR2 plasmid (Genewiz; Sigma-Aldrich; Merck KGaA) were transfected using Lipofectamine® 2000 reagent (Invitrogen; Thermo Fisher Scientific, Inc.) for 24 h at 37°C according to the manufacturer's instructions. The cells were starved in non-complemented RPMI media for 24 h. The conditioned media were harvested and centrifuged at 690 x g at room temperature to eliminate dead cells. The presence of extracellular AGR2 (eAGR2) was assessed using western blot analysis of media from non-transfected cells and transfected cells with pcDNA3.0 or pcDNA3.0/AGR2. The media were concentrated using Vivaspin 15R 5kDa following the manufacturer's protocol (Sartorius AG).

Recombinant AGR2. Recombinant AGR2 (RayBiotech, Inc.; cat. no. 230-00596) was reconstituted in 1X PBS at 20 μg/ml and used at 200 ng/ml to treat cells during senescence escape.

SA-β galactosidase staining. Cells were fixed for 10 min at room temperature in 1% formaldehyde, washed with PBS and incubated at 37°C for 16 h in the absence of CO_2 with freshly made staining solution: 0.3 mg/ml of 5-bromo-4-chloro-3-indolyl-β-d-galactopyranoside (X-Gal; Promega Corporation; cat. no. V394A), 40 mM citric acid (Sigma-Aldrich; Merck KGaA), 40 mM sodium phosphate (Sigma-Aldrich; Merck KGaA) [stock solution (400 mM citric acid, 400 mM sodium phosphate) held at pH 6], 5 mM potassium hexacyanoferrate (Sigma-Aldrich; Merck KGaA), 5 mM potassium ferricyanide (Sigma-Aldrich; Merck KGaA), 150 mM NaCl (Sigma-Aldrich; Merck KGaA) and 150 mM $MgCl_2$ (Sigma-Aldrich; Merck KGaA). SA-β galactosidase staining was observed using a light microscope (Life Technologies; EVOS XL Core) and images were captured at x40, x100 and x200 magnification in different areas in examples of each condition (31).

Western blotting. Following cell lysis with FASP Buffer (0.1 M Tris-HCL, 4% SDS, pH 7.6) containing a cocktail of inhibitors (10 μg/ml aprotinin, 10 μg/ml leupeptin, 10 μg/ml pepstatin, 1 mM Na3VO4, 50 mM NaF), lysates were sonicated for 20 sec at room temperature and then boiled for 10 min. Proteins were quantified using BCA kit (Thermo Scientific Inc.; Pierce Protein Assay kit cat. no. 23225) and 50 μg of each sample was separated on a SDS polyacrylamide gel (8 and 10% for AGR2, p21, p53, AKT, pAKT evaluation, 6% for RICTOR, pRICTOR evaluation) and transferred to a PVDF membrane. Following 1 h incubation in 5% milk (5% BSA for pRICTOR), Tris-buffered saline (TBS) and 0.1% Tween-20, the membranes were incubated overnight at 4°C with the following primary antibodies at 1:1,000:

AGR2 (Abnova; cat. no. 0001055-1-M03), Actin (Santa Cruz Biotechnology, Inc.; cat. no. sc-8432), AKT pan (Cell Signaling Technology, Inc.; cat. no. 2920S), phosphorylated (p)-AKT S473 (Cell Signaling Technology, Inc.; cat. no. 4058S), HSC70 (Santa Cruz, sc-7298), p21Waf1 (Cell Signaling Technology, Inc.; cat. no. 2947S), p53 (Santa Cruz, sc-98), p-p53 S15 (Cell Signaling Technology, Inc.; cat. no. 9286), RICTOR (Cell Signaling Technology, Inc.; cat. no. 2114T), p-RICTOR T1135 (Cell Signaling Technology, Inc.; cat. no. 3806S) and p-S6 ribosomal protein (S235/236) (Cell Signaling Technology, Inc.; cat. no. 2211). Membranes were then washed three times with TBS with 0.1% Tween 20 and incubated for 45 min with the secondary antibodies at 1:3,000: anti-rabbit IgG, horseradish peroxidase (HRP)-linked antibody (Cell Signaling Technology, Inc.; cat. no. 7074), anti-mouse IgG and HRP-linked antibody (Cell Signaling Technology, Inc.; cat. no. 7076). Visualization was performed by chemiluminescence with Fusion Solo (Vilber Lourmat) and quantification performed on Evolution Capt Solo (v 6 17.00) (Vilber Lourmat).

Flow cytometry. Data acquisition and analysis were performed on BD LSR II flow cytometry device and on Diva 6 software (BD Bioscience).

γ-H2AX (Ser 139) staining. A total of 250,000 cells (MCF7) were incubated with 4% paraformaldehyde at 37°C for 10 min and permeabilized with cold 90% methanol in ice for 30 min. Cells were then washed and incubated with 16 ng of A488 mouse anti-γ-H2AX (Ser 139) (BD Pharmingen; cat. no. 560445) or 16 ng of A488 mouse IgG1K (BD Pharmingen; cat. no. 557721) in the dark at room temperature for 1 h.

Cell cycle analysis. A total of 125,000 cells were incubated with 150 μl of solution A (trypsin 30 μg/ml; Sigma-Aldrich; Merck KGaA) at room temperature in the dark for 10 min. 125 μl of solution B (trypsin inhibitor 0.5 mg/ml, RNAse A 0.1 mg/ml; Sigma-Aldrich; Merck KGaA) was then added in the dark for 10 min. Finally, cells were incubated with 125 μl of solution C (propidium iodide 0.6 mM, spermine tetrahydrochloride 3.3 mM; Sigma-Aldrich; Merck KGaA) at 4°C for 10 min. All the solutions were prepared in a storage buffer pH 7.6 containing 3.4 mM sodium citrate $2H_2O$ (Sigma-Aldrich; Merck KGaA), 0.1% Igepal CA-630 (Sigma-Aldrich; Merck KGaA), 3 mM spermine tetrahydrochloride and 1 mM tris-aminomethane (32).

Patient samples. The research protocol was approved by the Institut de Cancerologie de l'Ouest Paul Papin (ICO, Angers, France) and written informed consent was obtained from all participating patients (approval number NCT02653105). A total of 74 samples were included in this protocol with patients' age range from 50 to 74 (recruitment date: March 2016). Tumor specimens were embedded in paraffin as normally performed for routine clinical analysis. Following histopathological diagnosis, the FFPE (Formalin-Fixed Paraffin-Embedded) tissues were sectioned at 20 μm, mounted on glass slides and compared with hematoxylin and eosin-stained (10 sec hematoxylin, 3 sec eosin, at room temperature) slides from the same block to identify tumor-rich tissue regions.

Sera from female patients with breast cancer were collected at the ICO in Angers between 2014 and 2017. All sera were collected following written informed consent. The study protocol was approved by UNICANCER (approval no. NCT00630032) and 197 patients >18 years old were included in this protocol. The sera were obtained from blood after centrifugation at 3,700 g at 4°C for 10 min, then stored at -80°C. All samples were obtained prior to surgery or neoadjuvant treatment.

AGR2 measurement by ELISA. The AGR2 concentration was determined using ELISA kit from USCN Life Science Inc. (ref. SEC285Hu). Briefly, sera were collected from healthy donor or patients with breast cancer by centrifugating blood samples at 4°C at 3,700 x g for 10 min, then diluted to 1:1,000 using 1X PBS before assay proceeding. Samples and standards were added into the provided microplates precoated with AGR2 antibody, before adding a biotin-conjugated antibody specific to AGR2. In the presence of avidin-conjugated HRP a color change occurred and the microplates were read in a Tecan microplate reader (Tecan Group, Ltd.) at 450 nm. The analysis was performed using Magellan software (version 7.0; Tecan Group, Ltd.; intra-assay coefficient <10%, inter-assay coefficient <12%).

Mass spectrometry
Creation of the spectral library. To build the spectral library, peptide solutions of several protein samples were analyzed by shotgun approach using micro-LC-MS/MS. A total of 5 pooled samples of breast tissues were prepared to obtain a good representation of the peptides. Each sample was fractionated by OFFGEL fractionator (3100 OFFGEL Fractionator; Agilent Technologies, Inc.) into 24 fractions. Each fraction was separated into a micro-LC system Ekspert nLC400 (Eksigent Technologies LLC) using a ChromXP C18CL column (0.3 mm x 15 cm, 3 μm, 120 Å; Eksigent Technologies LLC) at a flow rate of 5 μl/min. Water and acetonitrile, both containing 0.1% formic acid, were used as solvents A and B, respectively. The following gradient of solvent B was used: 0 to 5 min 5% B, 5 to 125 min 5 to 35% B, then 9 min at 95% B and finally 9 min at 5% B for column equilibration. As the peptides eluted, they were directly injected into a hybrid quadrupole-TOF mass spectrometer Triple TOF 5600+ (Sciex) operated with a 'top 30' data-dependent acquisition system using positive ion mode (pressure at the curtain plate: 60 psi without heating; flow rate 5 μl/min). The acquisition mode consisted of a 250 msec survey MS scan from 400 to 1,250 m/z, followed by an MS/MS scan from 200 to 1,500 m/z (75 msec acquisition time, 350 mDa mass tolerance, rolling collision energy) of the top 30 precursor ions from the survey scan. The peptide and protein identifications were performed using Protein Pilot software (version 5.0; Sciex) with a human Swiss-Prot/TrEMBL concatenated target-reverse decoy database (https://www.uniprot.org/, downloaded in March 2016) containing 142,441 human protein sequences, specifying MMTS as Cys alkylation. The false discovery rate (FDR) was set to 0.01 for both peptides and proteins. The MS/MS spectra of the identified peptides were then used to generate the spectral library for SWATH peak extraction using the add-in for PeakView Software (version 2.2, Sciex) MS/MSALL with SWATH Acquisition MicroApp (version 2.0, Sciex). Peptides with a confidence score above 99% were obtained from Protein Pilot database searches were included in the spectral library.

Table I. AGR2 concentrations in sera from healthy donors, patients with breast cancer and patients with breast cancer with metastasis.

Cases	Number	AGR2 mean concentration ng/ml	Standard deviation
Healthy donors	56	2.93	0.42
Patients with breast cancer	118	5.62	0.87
Patients with breast cancer and with metastasis	23	13.7	3.2

AGR2, anterior gradient 2.

Relative quantification by SWATH acquisition. MCF-7 cells were analyzed using a Data Independent Acquisition method (33). Each sample (5 μg) was analyzed using the LC-MS equipment and LC gradient described in the previous section following a SWATH-MS acquisition method. The method involved repeating the whole gradient cycle, which consisted of the acquisition of 35 TOF MS/MS scans of overlapping sequential precursor isolation windows (25 m/z isolation width, 1 m/z overlap, high sensitivity mode) covering the 400 to 1,250 m/z mass range, with a previous MS scan for each cycle. The accumulation time was 50 msec for the MS scan (400-1,250 m/z) and 100 msec for the product ion scan (230-1,500 m/z), making a 3.5 sec total cycle time.

Data analysis. The targeted data extraction of the SWATH runs was performed by PeakView using the MS/MSALL with SWATH Acquisition MicroApp. PeakView processed the data using the spectral library created from the shotgun data. Up to ten peptides per protein and seven fragments per peptide were selected, based on signal intensity; any shared and modified peptides were excluded from the extraction. The retention times from the peptides selected for each protein were realigned in each run according to the iRT peptides (Biognosys AG) spiked in each sample and eluting along the whole-time axis; the extracted ion chromatograms were generated for each selected fragment ion. PeakView computed a score and FDR for each assigned peptide using chromatographic and spectra components; only peptides with an FDR <5% were used for protein quantitation. The peak areas for peptides were obtained by summing the peak areas of the corresponding fragment ions; protein quantitation was calculated by summing the peak areas of the corresponding peptides. MarkerView (version 1.2; Sciex) was used for signal normalization and differential abundance was tested by applying a t-test at protein level.

GSEA Analysis. GSEA analysis was performed using GSEA software from Broad Institute (https://www.gsea-msigdb.org/gsea), the raw data tables were uploaded on the software. The data bases used are Hallmarks (h.all.v.7.0.symbol), Oncogenic signatures (C6.all.v.7.symbol) and Senescence signature (C2.CP.REACTOME.REACTOME_OXIDATIVE_STRESS_INDUCED_SENESCENCE).

Data deposition. The mass spectrometry proteomics data have been deposited to the ProteomeXchange Consortium via the PRIDE (http://www.proteomexchange.org/) (34) partner repository with the dataset identifier PXD014194 for breast cancer analysis and PXD028073 for emergent MCF7 analysis.

Statistical analysis. All data were expressed as mean ± standard deviation. Differences were analyzed using nonparametric tests (Mann-Whitney, Kolmogorov-Smirnov and one-way ANOVA with Dunnett's multiple comparison test). Pearson's correlation test was performed to assess the correlation between protein expression in breast cancer tumors. $P<0.05$ was considered to indicate a statistically significant difference.

Results

AGR2 is significantly overexpressed in sera of metastasized patients. Previous studies have shown that analysis of the proteome in colon and breast cancer makes it possible to identify proteins, such as OLFM4 and TSP1, that are involved in tumor progression and aggressiveness (9,10). Proteomic analysis of a cohort of colorectal tumors shows that AGR2 is expressed in colonic adenomas and that its expression is increased in the invasive stages of adenocarcinomas (stage IV) (9). AGR2 is involved in various cancer types, especially breast and prostate and is associated with poor prognosis (21,35).

To confirm these observations, the present study first evaluated the concentration of AGR2 in human serum samples from patients with breast cancer with or without metastasis and healthy controls using an ELISA approach. The results presented in Table I show that the mean value for healthy donors is 2.93±0.42 ng/ml (n=56), 5.62±0.87 ng/ml (n=118) in the breast cancer group and 13.7±3.2 ng/ml (n=23) in the breast cancer with metastasis group. AGR2 is significantly higher in patients with breast cancer with metastasis than healthy controls (P-value<0.0001; Fig. 1A; Table I).

Data were examined for the correlation between AGR2 and overall survival. Kaplan-Meier survival curves based on AGR2 expression were derived from Tang *et al* (36). This study compared the proteome of proteins extracted from breast tumors and adjacent noncancerous tissues by mass spectrometry. The cohort contained samples from the three molecular subtypes of breast cancer: Luminal A, HER2-positive and triple negative (36). The present study used the data on AGR2 expression from this breast cancer study to assess if overall survival can be related to AGR2. The results show that patients harboring high AGR2 expression present low survival compared to patients with low AGR2 expression (Fig. 1B; P-value=0.07).

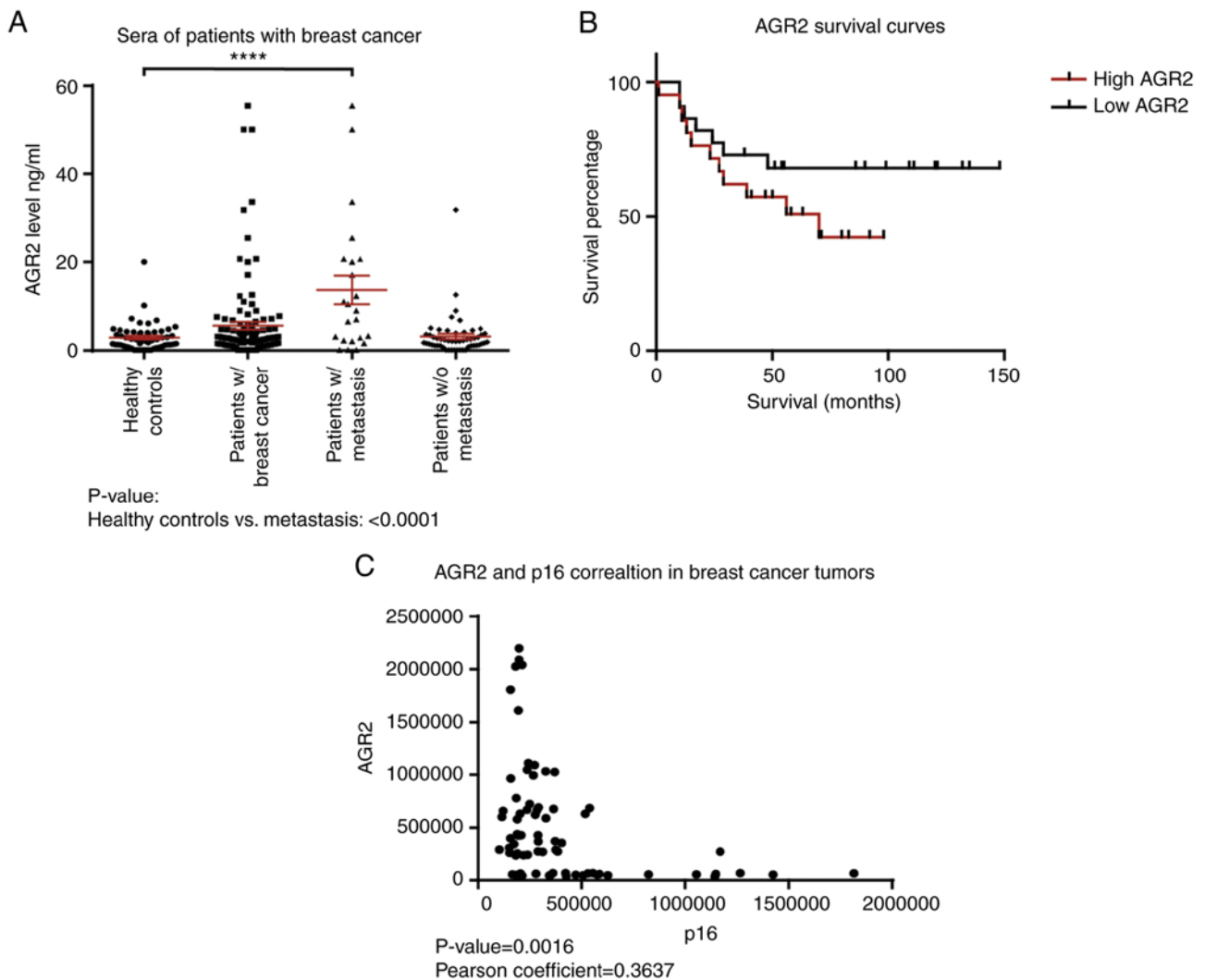To understand AGR2's implication in breast cancer progression, its correlation with tumor suppressors was

Figure 1. High AGR2 expression in patients with breast cancer is correlated with cancer progression, metastasis occurrence and low survival. (A) The AGR2 concentration was quantified in the sera of patients with breast cancer using an ELISA kit (number of patients with breast cancer=118) (****P<0.0001). (B) Kaplan-Meier survival curves based on AGR2 expression were obtained from data of Tang *et al* (36). (C) Correlation between the relative expressions of AGR2 and p16 proteins following a mass spectrometry analysis performed on tumors from patients with breast cancer (number of patients=119; P-value=0.0016). AGR2, anterior gradient 2; w/, with; w/o, without.

investigated using the SWATH-MS approach on 119 breast tumors. The results presented in Fig. 1C show that AGR2 expression is inversely correlated with p16, a major senescence regulator (P-value=0.0016). They suggest that AGR2 could induce tumor progression through the regulation of suppressive mechanisms such as senescence.

All these results showed that AGR2 was a protein detected in breast cancer. In addition, high concentration in the serum of patients was associated with a metastatic state and its expression in breast tumors is associated with poor prognosis.

AGR2 is overexpressed during senescence escape. In breast and colorectal cell lines, it was shown that genotoxic treatment induced senescence. As depicted in Fig. 2A, doxorubicin (25 ng/ml) and sn38 (5 ng/ml) were used to treat respectively the MCF-7 and LS174T cell lines for 96 h. CIS was confirmed using p21WAF1 expression (Fig. 2A, upper left) and SA-β-galactosidase (Fig. 2A, upper right.). These experiments revealed that both MCF-7 and LS174T cells showed upregulation of the cell cycle inhibitor p21 and high SA-β-galactosidase

staining. The MCF-7 cell line also showed an elevation in γ-H2AX staining, which reflected an increase in DNA damage (Fig. 2A, lower part).

The present authors recently reported that breast and colorectal cells can adapt to CIS and resume proliferation. CIS escape generates heterogeneous populations called emerging cells and comprising senescent cells and dividing cells (37). Taking into account the results obtained from proteomic analysis and the anticorrelation between AGR2 and p16, AGR2 expression was analyzed during CIS induction and CIS escape in emerging cells (Fig. 2B, upper part). AGR2 expression was first analyzed in the two CIS escape models. Analysis of the MCF-7 model shows that expression of the protein AGR2 (Fig. 2B, left) and its mRNA (Fig. 2C) was induced in the emerging population but not in senescent cells. Whereas in the LS174T model, western blot analysis shows no significant variation in AGR2 expression between senescent and emergent cells. To analyze AGR2 expression more accurately in the LS174T model, mass spectrometry analysis was performed to compare senescent and emergent cells. The result showed
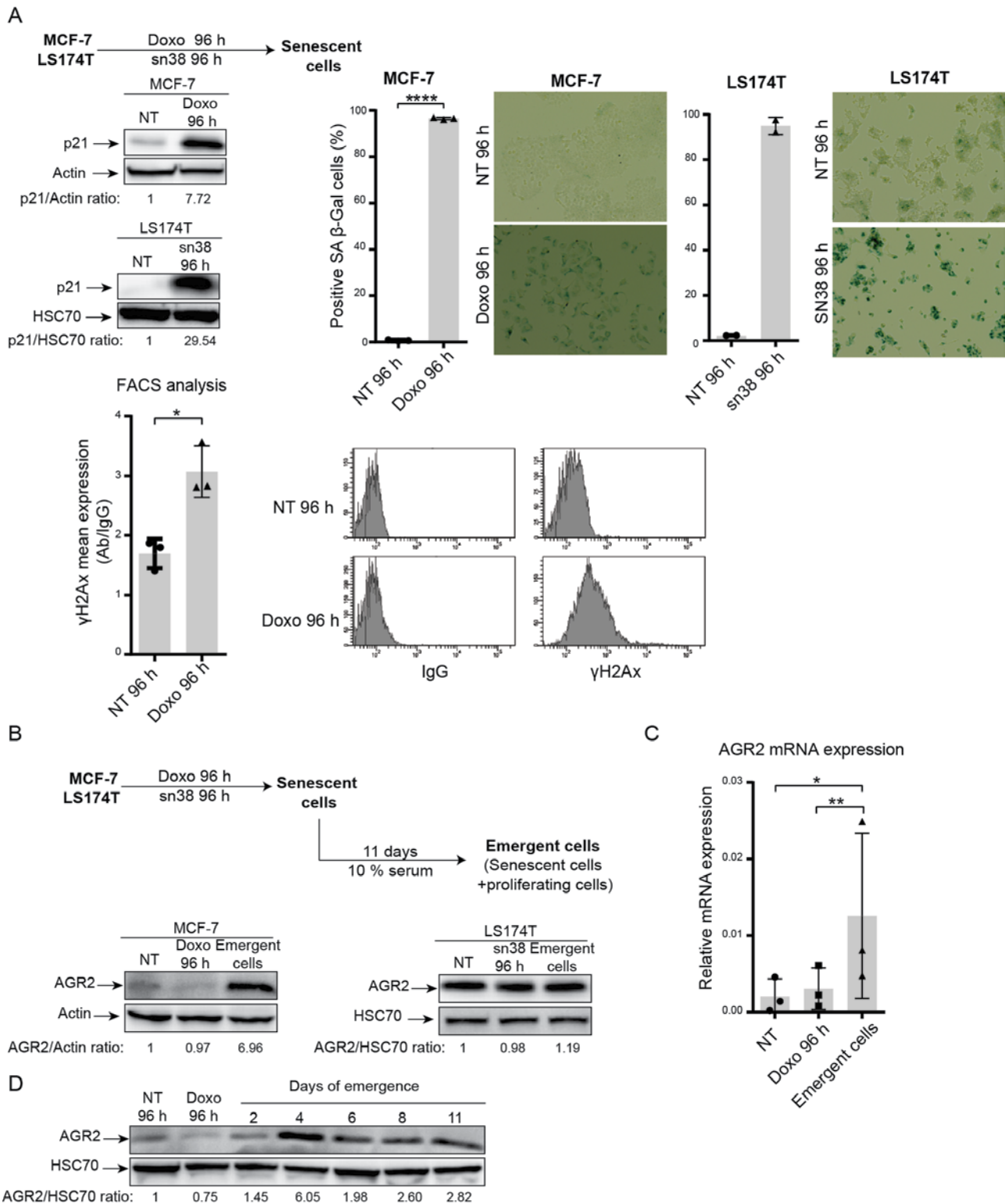
Figure 2. Chemotherapy induces MCF-7 and LS174T cell senescence and AGR2 is overexpressed during CIS escape. (A) Senescence was induced in MCF-7 breast cancer cell line following doxorubicin treatment (25 ng/ml) for 96 h and in the colorectal cell line LS174T following sn38 treatment (5 ng/ml) for 96 h. The senescent state was evaluated by p21 expression using western blotting and β-galactosidase staining (MCF-7 n=3 ± standard deviation, *P-value=0.0152); LS174T n=2 ± standard deviation; magnification, x400) and DNA damage using FACS quantification of γ-H2AX staining (n=3 ± standard deviation, *P-value<0.0001). AGR2 expression was evaluated using (B) western blotting (MCF-7 n=3; LS174T n=3) and (C) quantitative PCR (n=3 ± standard deviation, *P-value=0.385, **P-value=0.0085) in non-treated, senescent and emergent cells. (D) The kinetic of AGR2 expression during cell emergence was assessed by western blotting (n=3). AGR2, anterior gradient 2; CIS, chemotherapy-induced senescence.

a slight increase in AGR2 expression in emergent LS174T compared to senescent LS174T (data not shown). Finally, AGR2 expression during CIS escape was assessed with two days' interval. The result presented in Fig. 2D showed that AGR2 expression during CIS escape increased after four days of emergence.
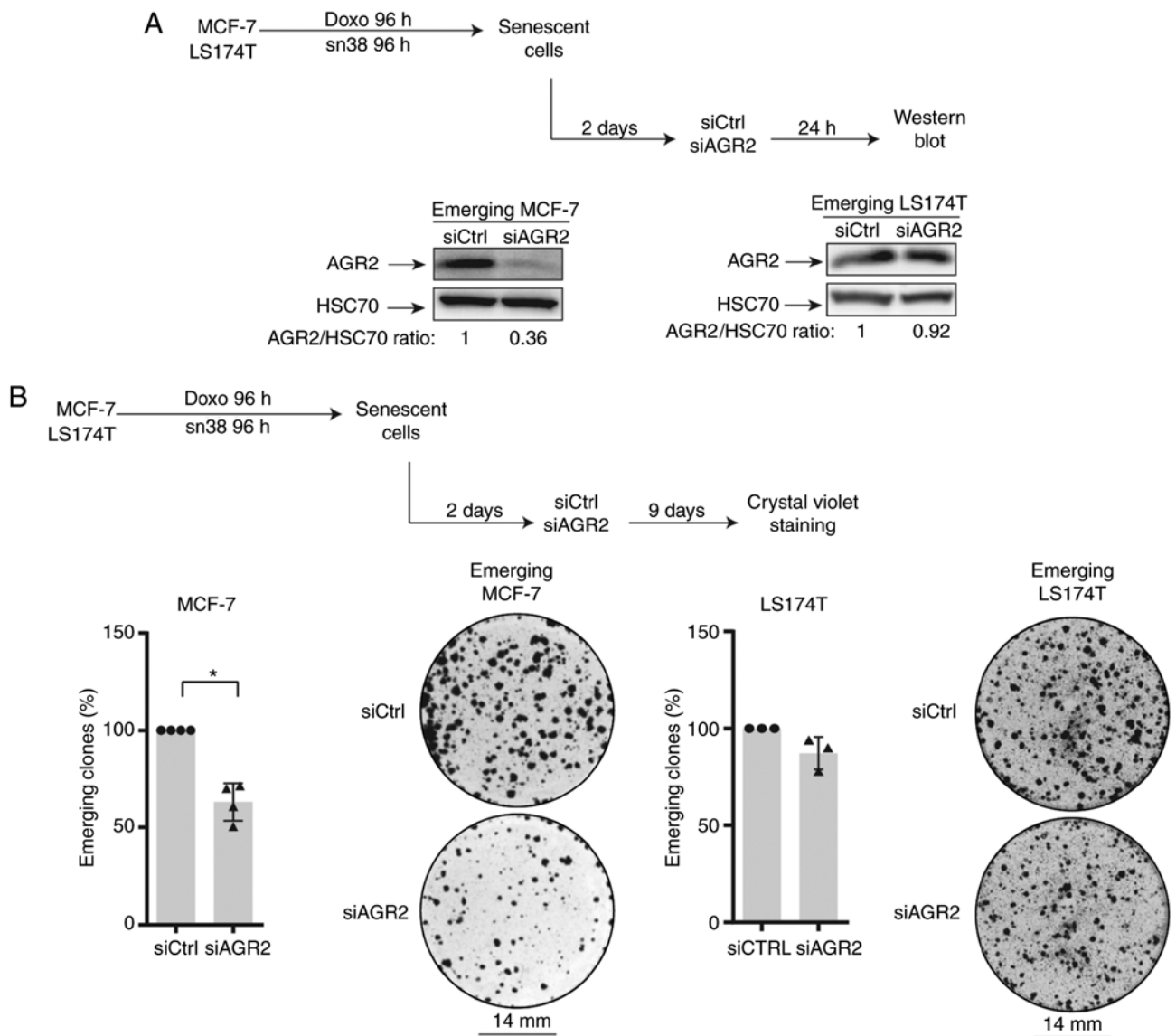
Figure 3. AGR2 suppression prevents CIS escape. (A) Western blotting validation of AGR2 down-expression following siRNA transfection after two days of emergence (n=3). (B) Cell emergence was evaluated by colony counting, after siRNA transfection, following crystal violet staining (MCF-7 n=4 ± standard deviation, *P-value=0.0286; LS174T n=3). AGR2, anterior gradient 2; CIS, chemotherapy-induced senescence; si, small interfering.

These initial results led to study AGR2's potential role in CIS escape, primarily by inhibiting its expression or adding its extracellular form.

AGR2 inhibition prevents CIS escape. To evaluate AGR2's involvement in CIS escape, its expression was inhibited in senescent cells. For this, siRNA was transfected two days after the end of treatment (in accordance with the kinetic of expression) as specified in Fig. 3A (top). Western blot analysis confirmed the protein's downregulation (Fig. 3A, lower left). The impact of AGR2 inhibition on the number of emerging clones was then evaluated (Fig. 3B, upper part). As shown in Fig. 3B (left lower part), AGR2 downregulation significantly decreased the percentage of emerging clones.

The present study also transduced the siRNA against AGR2 into emerging colorectal cell line. It was not possible to inhibit AGR2 expression efficiently due to the high amount of protein (Fig. 3A, lower right). However, a slight decrease in the number of proliferating clones was observed following siRNA transduction during the emergence of LS174T cell line (Fig. 3B, right).

Taken together these results indicated that AGR2 expression favors cell emergence after CIS. This effect is heterogenous and seems to depend on AGR2 expression on cell lines. Although a slight decrease in the number of emerging clones was observed after siRNA transfection in colorectal cells, the present study chose to investigate the CIS escape mechanism only in the breast cancer model.

eAGR2 enhances CIS escape in MCF-7 cells. To confirm the role of AGR2 in CIS escape, a plasmid construct coding for AGR2 protein was transduced into emerging MCF-7. This experiment could not be of a use as the transduction lead to cell death. Therefore, the present study chose to assess the role of extracellular AGR2 on CIS escape.

Previous studies have shown that the extracellular form of AGR2 (eAGR2) is implicated in the proliferation
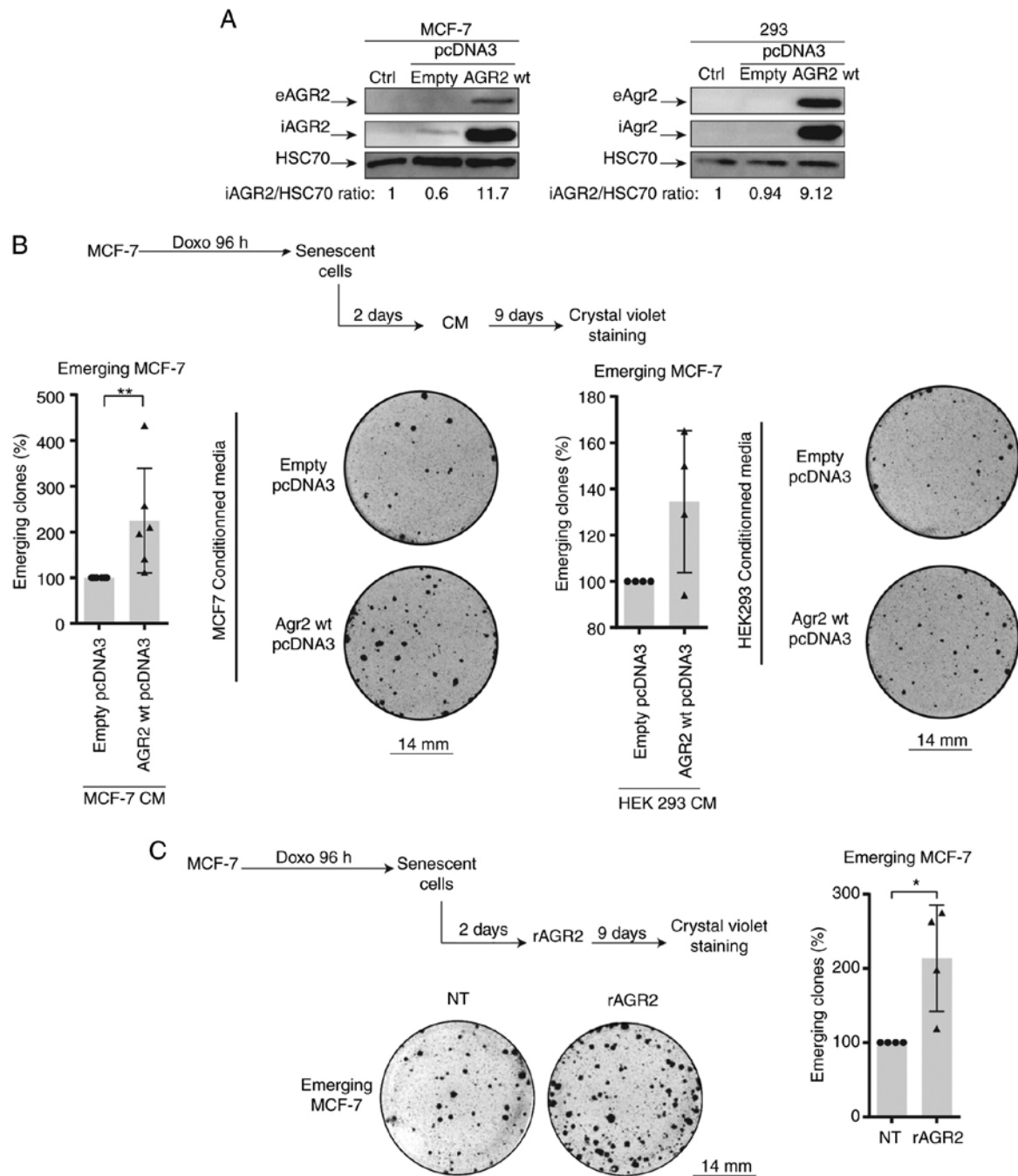
Figure 4. Soluble AGR2 favors CIS escape. (A) Conditioned media were generated from MCF-7 and 293 transfected with either pcDNA3.0 or pcDNA3.0 AGR2 wt. eAGR2 expression in the media was assessed through western blotting. (B) Emerging MCF-7 were treated at day two of emergence with the conditioned media. The number of emerging clones was evaluated with crystal violet staining after eleven days of emergence (CM from MCF-7: n=6 ± standard deviation, **P-value=0.0022; CM from 293: n=4 ± standard deviation). (C) Emerging MCF-7 were treated at day two of emergence with recombinant human AGR2 at 200 ng/ml. The emerging clones were revealed by crystal violet staining after 11 days of emergence (n=4 ± standard deviation, *P-value=0.0286). AGR2, anterior gradient 2; iAGR2, intracellular AGR2; CIS, chemotherapy-induced senescence; wt, wild type; eAGR2, extracellular AGR2; rAGR2, recombinant AGR2; NT, non-treated.

and aggressiveness of tumor cells (15,17). Therefore the effect of eAGR2 on CIS escape was studied. For this, the growing MCF-7 cells and 293 cells were transfected with a plasmid-encoding AGR2 or with a control plasmid. After two days of transfection, the culture media was collected and added to MCF-7 senescent cells. eAGR2 production was monitored by western blotting (Fig. 4A). eAGR2 significantly increases the number of emergent clones, as shown in Fig. 4B. Recombinant eAGR2 (200 ng/ml) was

also added during CIS escape (Fig. 4C, upper left). The count of emerging clones showed that the recombinant molecule significantly increased CIS escape (Fig. 4C, right and lower part).

The effect of eAGR2 on CIS escape after inhibition AGR2 expression was also assessed using siRNA. This experiment showed no influence of eAGR2 on cell emergence (data not shown), thus eAGR2 alone is not sufficient to favor CIS escape and a cooperation is needed between its two forms.

Table II. Molecular signatures that are significantly deregulated following AGR2 suppression.

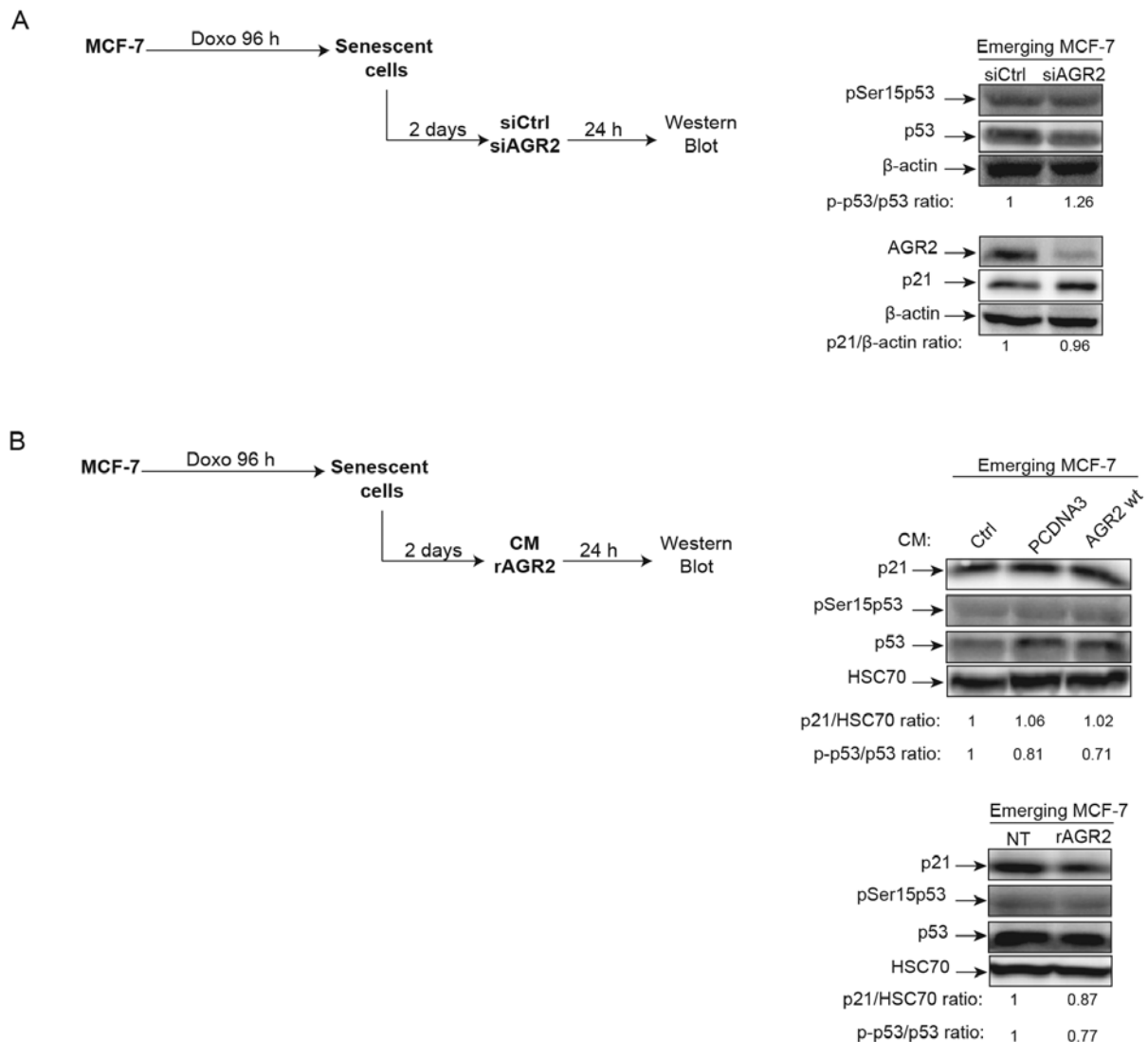| Database (https://www.gsea-msigdb.org/gsea)	Signatures	Number of proteins	P-value	FDR q-value
Hallmarks (h.all.v7.0. symbols)	HALLMARK_UNFOLDED_PROTEIN_RESPONSE	41	0.01988	0.25301
	HALLMARK_PI3K_AKT_MTOR_SIGN ALING	27	0.04490	0.53485
Oncogenic signatures (c6.all.v7.0.symbols)	MTOR_UP.N4.V1_UP	30	<0.001	0.00820
	MTOR_UP.V1_UP	33	<0.001	0.03366
	AKT_UP.V1_UP	20	0.01362	0.15083
	GCNP_SHH_UP_LATE.V1_UP	37	0.03137	0.14104
	CYCLIN_D1_UP.V1_UP	22	0.01183	0.16396
	NRL_DN.V1_DN	17	0.02236	0.27494
Senescence signature	REACTOME_OXIDATIVE_STRESS_INDUCED_SENESCENCE	7	0.03400	0.03600

FDR, false discovery rate.

Figure 5. AGR2 does not regulate the p53/p21 pathway during cell emergence. (A) The expression of senescence markers phosphoSer15-p53 and p21 was evaluated using western blotting on emergent cells transfected with siRNA directed against AGR2 (n=3). (B) The expression of senescence markers phosphoSer15-p53 and p21 was evaluated using western blot on emergent cells following treatment with conditioned media expressing AGR2 (n=3) or with recombinant AGR2 (200 ng/ml; n=3). AGR2, anterior gradient 2; si, small interfering; rAGR2, recombinant AGR2; wt, wild type; si, small interfering; Ctrl, control; p-, phosphorylated.
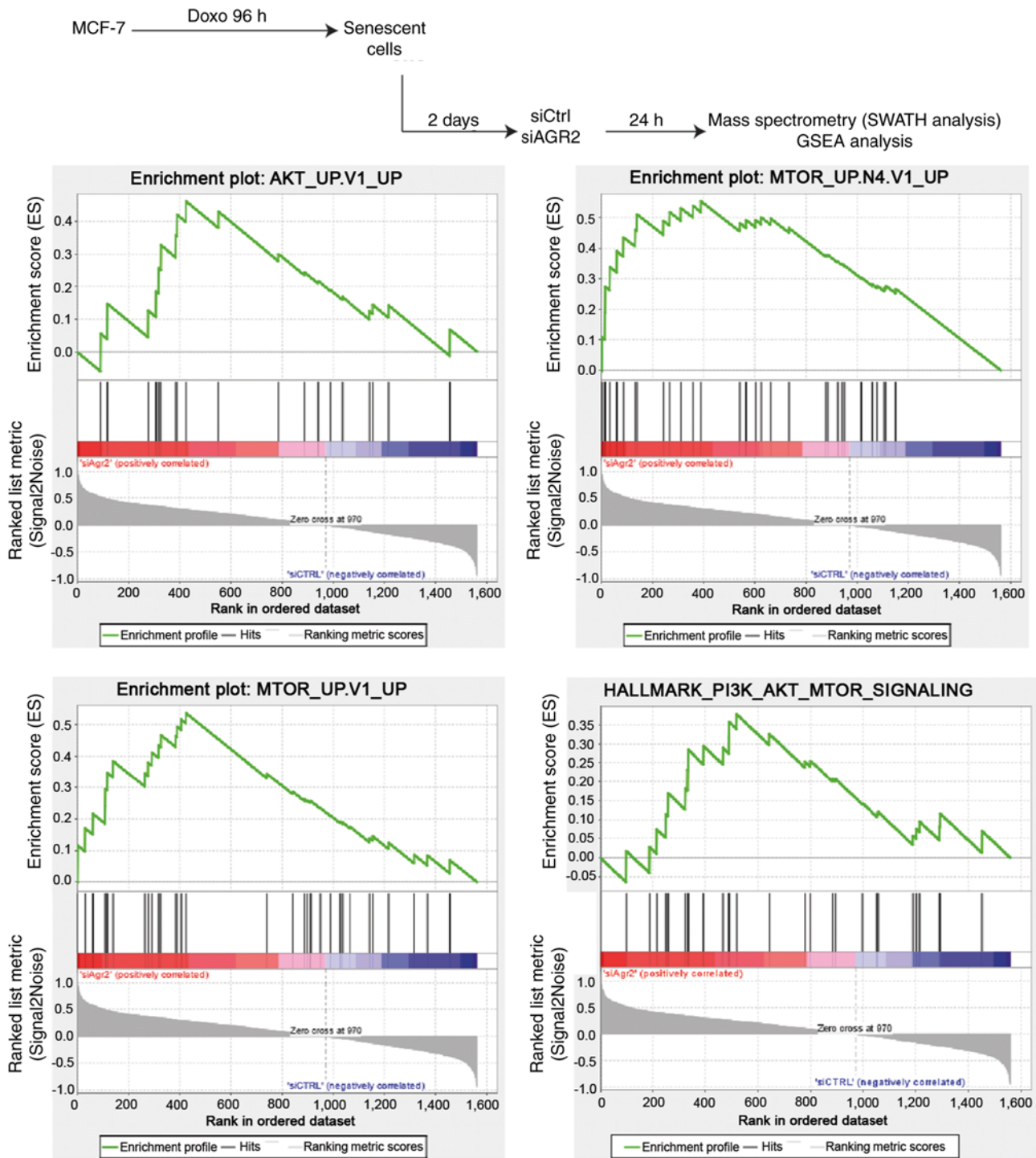
Figure 6. AKT and mTOR pathways are deregulated following AGR2 suppression during CIS escape. GSEA was performed on the proteomes obtained from emergent cells transfected with control siRNA (right part of the plots) or siAGR2 (left part of the plots). mTOR, mammalian target of rapamycin; AGR2, anterior gradient 2; CIS, chemotherapy-induced senescence; GSEA, Gene Set Enrichment Analysis; si, small interfering; Ctrl, control.

AGR2 does not regulate p21/p53 during CIS escape. In light of AGR2's observed effects on senescence escape, whether this effect is regulated or not by the p21/p53 signaling pathway was investigated. Indeed, several studies have shown that AGR2 may regulate p53 activation following DNA damage by UV or genotoxic treatments. In these studies, suppression of AGR2 leads to higher p53 activation by allowing phosphory-lation of serine 15 (38,39). Based on these observations, the effect of AGR2 on the phosphorylation of p53 on serine 15 and the expression of its target gene p21 was assessed during senescence escape. To this end, senescent MCF-7 cells were transfected with a siRNA directed against AGR2, the cells recovered after 24 h (Fig. 5A, left) and activation of the p53/p21 pathway analyzed. However, neither the phosphorylation level of p53 serine 15 nor the level of p21 expression were modified by the inhibition of AGR2 expression (Fig. 5A, right). The same results were obtained when senescent MCF-7 cells were stimulated by extracellular AGR2 (Fig. 5B, left) CM (Fig. 5B,
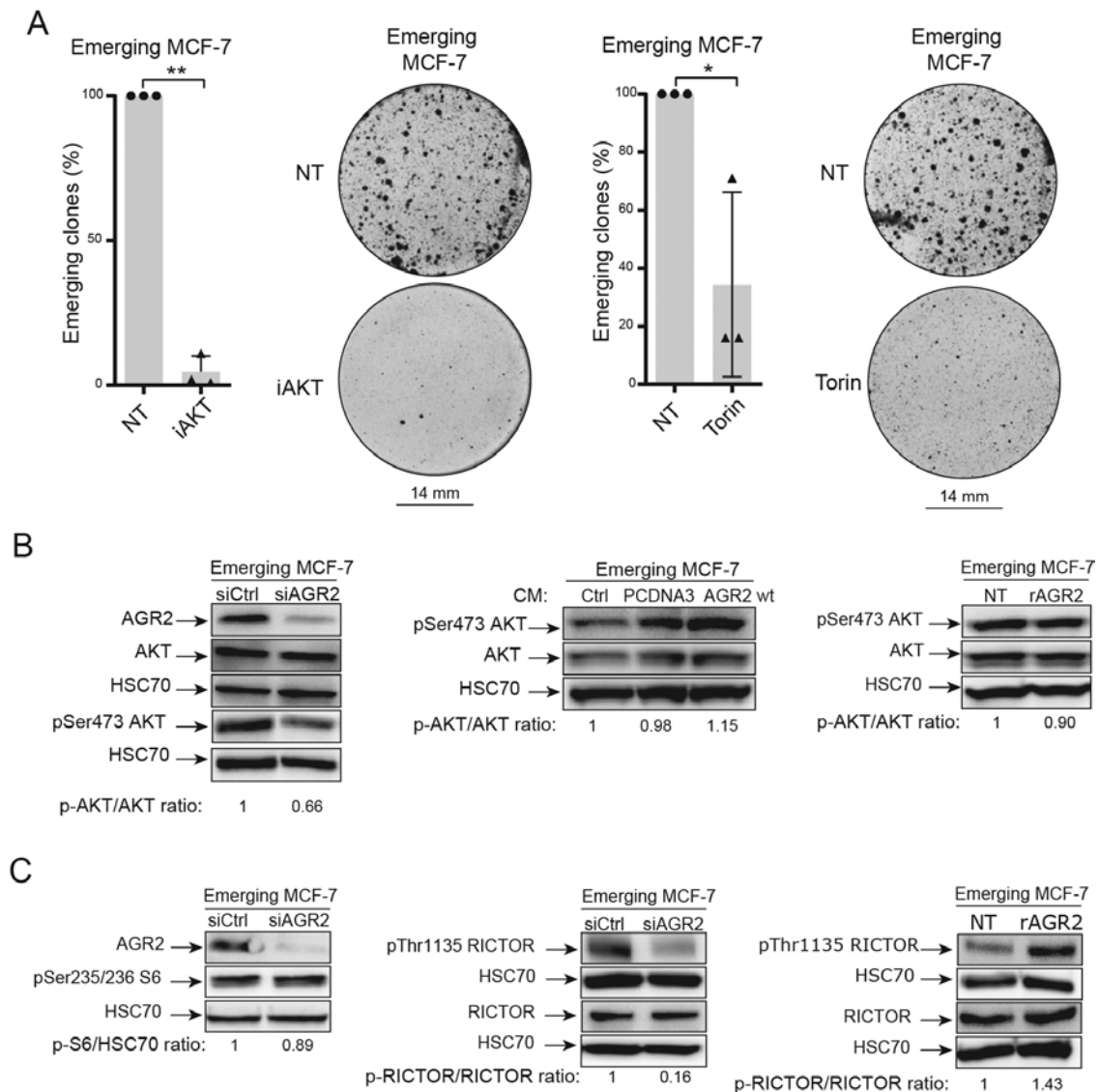
Figure 7. AGR2 acts through the AKT signaling pathway during CIS escape. (A) Cell emergence was measured by colony counting after iAKT treatment (100 μM; n=3 ± standard deviation; [**]P-value=0.0011) and Torin treatment (10 nM; n=3 ± standard deviation; [*]P-value=0.0231) (B) The phosphorylation of AKT protein on emergent cells transfected with siAGR2 or treated with soluble AGR2 (CM and rAGR2) was assessed after two days of emergence using western blotting (n=3). (C) The phosphorylation of S6 and RICTOR after AGR2 suppression or eAGR2 and rAGR2 treatment in emergent cells was evaluated using western blotting following two days of emergence (n=3). AGR2, anterior gradient 2; CIS, chemotherapy-induced senescence; si, small interfering; iAKT, inhibitor of AKT; eAGR2, extracellular AGR2; rAGR2, recombinant AGR2; NT, non-treated; p-, phosphorylated.

upper right) or recombinant (r)AGR2 (Fig. 5B, lower right). These results show that AGR2 does not modify the p53/p21 pathway during emergence.

AGR2 facilitates senescence escape by regulating the mTOR/AKT pathway. To investigate new pathways by which AGR2 could control the emergence of MCF-7 cells, a proteomic analysis was performed using SWATH-MS as previously described (40). Gene Set Enrichment Analysis (GSEA) of proteomes from emergent MCF-7 transduced with siRNA directed against AGR2 or control siRNA allowed the identification of pathways that are significantly correlated with the loss of AGR2 during emergence (Fig. 6, upper part). This analysis revealed only two gene sets from the Hallmarks database with a nominal P-value <0.05 and a FDR >25%. However, assessing the oncogenic signature database revealed seven

significantly enriched gene sets (P-value <0.05), including five with a FDR <25% (Table II). The enriched gene sets in the results were related to AKT and mTOR signaling pathways, suggesting that AGR2 could regulate these pathways during emergence (Fig. 6, lower part).

Previous studies in the authors' laboratory have shown that these two pathways are involved in CIS escape (7). Therefore, AKT and mTOR pathways were inhibited using two inhibitors (iAKT1/2 and Torin). The results presented in Fig. 7A show that these inhibitors prevented CIS escape.

The present study first focused on the AKT pathway. The importance of AKT phosphorylation (Ser 473) during CIS escape has been previously shown (7). The results led to the study of this phosphorylation when AGR2 expression was modulated. When AGR2 expression was inhibited by siRNA in senescent MCF-7 cells, a decrease in AKT phosphorylation on its serine 473 residue
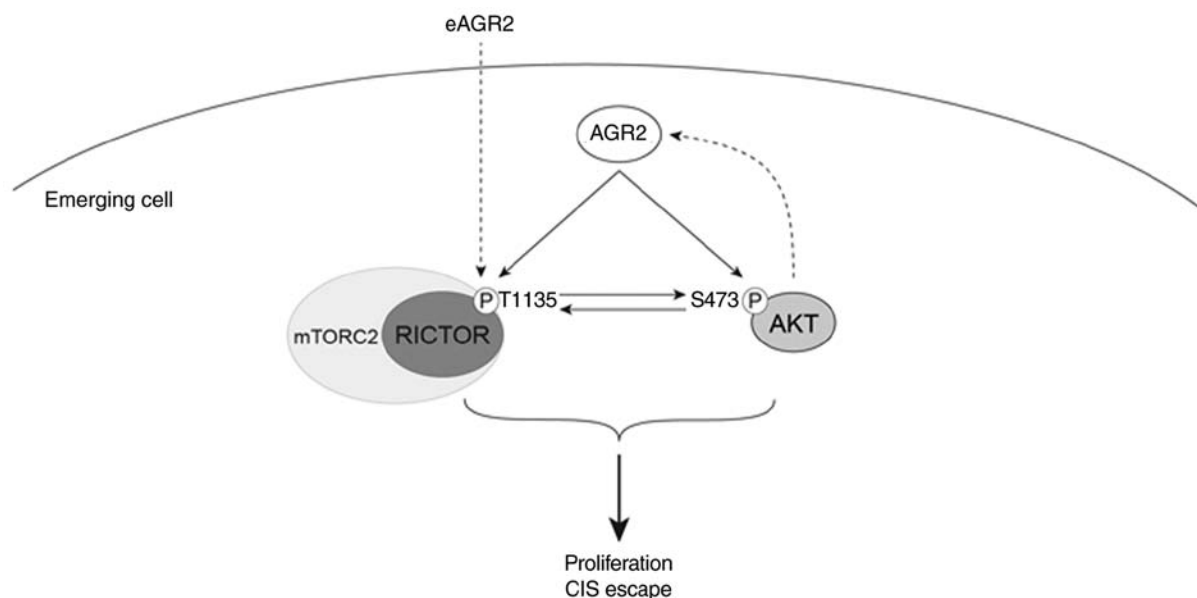
Figure 8. AGR2 upregulation during emergence induces AKT and RICTOR activation via phosphorylation. During CIS escape, AGR2 expression is induced and allows the phosphorylation of both AKT and RICTOR. The two pathways are known to contribute to cell proliferation. RICTOR activation might also be induced by the extracellular AGR2. AGR2, anterior gradient 2; CIS, chemotherapy-induced senescence; mTORC, mammalian target of rapamycin complex; eAGR2, extracellular AGR2.

was observed (Fig. 7B, left). However, AKT phosphorylation was not increased by extracellular forms of AGR2 [conditioned media, Fig. 7B (middle) and rAGR2, Fig. 7B (right)].

Several studies show that AKT phosphorylation is regulated by the mTOR pathway (41-43). The proteomic study identified the mTOR signaling pathway as being regulated by AGR2 during CIS escape. It was therefore determined if mammalian target of rapamycin complex mTORC1 and mTORC2 were regulated by AGR2 during CIS escape. First, one of the main targets of mTORC1, the ribosomal protein S6 was studied. The results presented in Fig. 7C (left) show that siRNA-mediated inhibition of AGR2 in senescent cells did not change S6 phosphorylation. The total form of S6 was not analyzed as variation of its phosphorylated form was not observed.

Given these results, the regulation of other mTOR signaling pathways by AGR2 were studied. The activation of mTORC2 complex is attested by the phosphorylation of RICTOR on threonine 1135. The western blotting results presented in Fig. 7C (middle) show a decrease in RICTOR phosphorylation when AGR2 was inhibited by siRNA. Conversely, RICTOR phosphorylation on Thr1135 level is higher when MCF-7 cells are stimulated with eAGR2 (Fig. 7C, right). Taken together, the results showed that AGR2's effect on CIS escape could be mediated by activation of the mTORC2/AKT signaling pathway.

Discussion

Chemotherapy-induced senescence is a complex mechanism which has been described as a first step in tumor cell proliferation arrest and elimination by the immune system (44). Long considered irreversible, this mechanism is being called into question (1,6). It has been shown in different cell types, notably in a breast cancer model, that cells treated with doxorubicin go into senescence. Some of these cells are able to emerge after chemotherapy and reproliferate (7,8). This observation

suggests that the phenomenon can be considered as therapeutic failure or treatment resistance. The present study aimed to identify and establish new proteins and pathways involved in the induction of CIS escape. Given the proteomic studies in patients with breast cancer and the proteins identified the present study focused on the protein AGR2.

In breast cancer tumors, AGR2 is overexpressed and serves a major role in cell proliferation and aggressiveness. It has been shown that AGR2 expression in breast cancer cell lines induces proliferation through the regulation of a number of proliferative proteins (26). AGR2 is also known as a tumor aggressiveness marker and its overexpression leads to metastasis induction (27). However, among the number of studies published on the role of AGR2 in tumor progression (15,21,26,45,46), none refers to its contribution to chemotherapy-induced senescence and particularly the escape leading to tumor cell proliferation.

The present study showed for the first time that the presence of AGR2 in the sera of patients with breast cancer is a marker of metastasis and that its expression in breast tumors is inversely correlated to p16 expression. It also highlighted that AGR2 is involved in the emergence of cells after senescence induction by doxorubicin. The present study underlined that AGR2 was detectable in the serum of untreated patients with breast cancer and that its level was significantly higher in patients compared to healthy donors. In addition, the amounts of AGR2 were significantly higher in the metastatic patient group. From these observations the present study demonstrated that AGR2 is anticorrelated with p16, a marker of cellular senescence as has been shown in ovarian cancer (47) and therefore it studied the potential role of AGR2 during CIS and implication in the appearance of emerging clones.

AGR2's role in senescence is not known. Although one study showed that its loss induces the senescence of prostate tumor cells (48), there is no research on AGR2's potential role in the different forms of senescence, especially during CIS.

The present study proposed in its CIS escape model that AGR2 serves an important role and that this action is mediated by the cellular and secreted forms of the molecule. Indeed, it showed that the loss of AGR2 in senescent cells induced a loss of the number of emergent clones, but that the contribution of the extracellular form (eAGR2) made it possible to increase the number of reproliferate clones. Mass spectrometry proteomic approaches demonstrated that the role of AGR2 is linked to the mTORC and AKT signaling pathways. Indeed, the AKT signaling pathway is involved in CIS escape (7). Furthermore, AKT is implicated in AGR2 regulation following tamoxifen treatment, leading to cell invasion (49). It is also shown that AGR2 knockdown reduces chemotherapy resistance by negatively regulating AKT/ERK signaling pathways and promoting apoptosis (50,51). The present study then evaluated this pathway's activation in the model and the results showed that AGR2 suppression during CIS escape led to a decrease in AKT phosphorylation on Ser473. Moreover, it has been shown that mTORC1 regulates AGR2 expression by regulating the length of its mRNA (52). The CIS escape model of the present study investigated the potential feedback regulation between mTORC1 and AGR2 by assessing the protein S6 phosphorylation. The results showed no modification in the activation of mTORC1 signaling pathway following AGR2 suppression during cell emergence. It has been shown that mTORC2 is regulated by AGR2 through the phosphorylation of RICTOR (53). The present study then also analyzed this pathway's activation in its model. The results showed that AGR2 suppression during CIS escape led to a reduction in RICTOR phosphorylation on Threonine 1135. By contrast, the stimulation of emerging cells by recombinant AGR2 induced RICTOR phosphorylation. These results suggested that AGR2 induced the proliferation of senescent cells by activating AKT and mTORC2 signaling, independently of the p53/p21 pathway (Fig. 8). However, the role of AGR2 in CIS escape was only confirmed in a breast cancer cell line and only a slight effect was observed in a colorectal cell line. This limitation needs more investigations using other breast and colorectal cell lines expressing AGR2 moderately, to inhibit efficiently its expression.

Altogether, the findings of the present study demonstrated that AGR2 could be used as a blood marker of metastasis and is a poor prognostic biomarker in patients with breast cancer. It also showed that AGR2 is implicated, by its secreted and intracellular form, in senescence escape via the activation of new signaling pathways. From these conclusions, measuring AGR2 concentration in patients could help predict tumor progression and prevent potential relapse following chemotherapy treatment.

AGR2 is known to interact with several proteins, which allows it to participate in different mechanisms (13). This feature should be explored in the model of the present study, using co-immunoprecipitation combined with mass spectrometry, to determine the AGR2 partners responsible for CIS escape induction. Furthermore, it would be useful to examine whether AGR2 interacts directly with AKT and RICTOR to induce their phosphorylation. Finally, AGR2 is also known to be implicated in endoplasmic reticulum stress and UPR (Unfolded Protein Response) pathways (54). AGR2 is overexpressed during endoplasmic reticulum stress in pancreatic cells and contributes to removing that stress by activating UPR proteins such as binding immunoglobulin protein and X antigen binding protein 1 (55). Given these observations, AGR2 might be a key protein to link UPR pathways to CIS escape. Therefore, AGR2 expressed during CIS escape can accelerate endoplasmic stress repair, allowing good protein folding and more cell proliferation. Conversely, AGR2 expressed during CIS escape can be a consequence of UPR pathways activation, which can lead to the activation of proliferative pathways such as AKT and mTORC2 and so promote cell proliferation. Moreover, it has been shown that AGR2 can be found in the cell in monomeric and dimeric forms, with this balanced status giving AGR2 new functions (17). In the model of the present study, the dimeric form should be assessed to determine whether during CIS escape AGR2 promotes proliferation as a monomeric or dimeric form.

The present study performed proteomic analysis (ELISA and SWATH-MS) on patient samples to study AGR2 expression and its outcome in breast cancer. On the other side, a CIS escape model was used to study the role of AGR2 in senescence escape and the pathways it regulates. Through the results obtained *in vivo* and *in vitro* it is possible to understand how cells are able to escape tumors suppression and which pathways are upregulated to permit cell proliferation.

Availability of data and materials

The datasets used and/or analyzed during the current study are available from the corresponding author on reasonable request.

Authors' contributions

AM and EL conceived and designed the experiments with assistance from OC. AM performed and interpreted the experiments. AB and CH performed ELISA assay on sera samples and prepared breast cancer, and MCF7 cells samples for mass spectrometry analysis. CG performed proteomic analysis on mass spectrometer and analyzed raw data and performed statistical analysis of ELISA assay data. AM performed GSEA analysis with the assistance of CG. AM and EL wrote, reviewed, and revised the manuscript with assistance of OC and CG. AM, EL and GL performed experiments for reviewing process. AM, EL, and CG confirm the authenticity of all data. All authors read and approved the final manuscript.

Ethics approval and consent to participate

Written consent was obtained from patients upon registration in the experimental protocol by Institut de Cancérologie de l'Ouest.

Patient consent for publication

Not applicable.

Competing interests

The authors declare that they have no competing interests.

References

1. Lee S and Schmitt CA: The dynamic nature of senescence in cancer. Nat Cell Biol 21: 94-101, 2019.
2. Rodier F, Coppé J, Patil CK, Hoeijmakers WA, Muñoz DP, Raza SR, Freund A, Campeau E, Davalos AR and Campisi J: Persistent DNA damage signalling triggers senescence-associated inflammatory cytokine secretion. Nat Cell Biol 11: 973-979, 2009.
3. Beauséjour CM, Krtolica A, Galimi F, Narita M, Lowe SW, Yaswen P and Campisi J: Reversal of human cellular senescence: Roles of the p53 and p16 pathways. EMBO J 22: 4212-4222, 2003.
4. Kuilman T and Peeper DS: Senescence-messaging secretome: SMS-ing cellular stress. Nat Rev Cancer 9: 81-94, 2009.
5. te Poele RH, Okorokov AL, Jardine L, Cummings J and Joel SP: DNA damage is able to induce senescence in tumor cells in vitro and in vivo. Cancer Res 62: 1876-1883, 2002.
6. Narita M, Nũnez S, Heard E, Narita M, Lin AW, Hearn SA, Spector DL, Hannon GJ and Lowe SW: Rb-mediated heterochromatin formation and silencing of E2F target genes during cellular senescence. Cell 113: 703-716, 2003.
7. Vétillard A, Jonchère B, Moreau M, Toutain B, Henry C, Fontanel S, Bernard AC, Campone M, Guette C and Coqueret O: Akt inhibition improves irinotecan treatment and prevents cell emergence by switching the senescence response to apoptosis. Oncotarget 6: 43342-43362, 2015.
8. Jonchère B, Vétillard A, Toutain B, Lam D, Bernard AC, Henry C, De Carné Trécesson S, Gamelin E, Juin P, Guette C and Coqueret O: Irinotecan treatment and senescence failure promote the emergence of more transformed and invasive cells that depend on anti-apoptotic Mcl-1. Oncotarget 6: 409-426, 2015.
9. Besson D, Pavageau AH, Valo I, Bourreau A, Bélanger A, Eymerit-Morin C, Moulière A, Chassevent A, Boisdron-Celle M, Morel A, *et al*: A quantitative proteomic approach of the different stages of colorectal cancer establishes OLFM4 as a new nonmetastatic tumor marker. Mol Cell Proteomics 10: M111.009712, 2011.
10. Campone M, Valo I, Jézéquel P, Moreau M, Boissard A, Campion L, Loussouarn D, Verriele V, Coqueret O and Guette C: Prediction of recurrence and survival for triple-negative breast cancer (TNBC) by a protein signature in tissue samples. Mol Cell Proteomics 14: 2936-2946, 2015.
11. Persson S, Rosenquist M, Knoblach B, Khosravi-Far R, Sommarin M and Michalak M: Diversity of the protein disulfide isomerase family: Identification of breast tumor induced Hag2 and Hag3 as novel members of the protein family. Mol Phylogenet Evol 36: 734-740, 2005.
12. Park SW, Zhen G, Verhaeghe C, Nakagami Y, Nguyenvu LT, Barczak AJ, Killeen N and Erle DJ: The protein disulfide isomerase AGR2 is essential for production of intestinal mucus. Proc Natl Acad Sci 106: 6950-6955, 2009.
13. Delom F, Mohtar MA, Hupp T and Fessart D: The anterior gradient-2 interactome. Am J Physiol Cell Physiol 318: C40-C47, 2020.
14. Delom F, Nazaraliyev A and Fessart D: The role of protein disulphide isomerase AGR2 in the tumour niche. Biol Cell 110: 271-282, 2018.
15. Fessart D, Domblides C, Avril T, Eriksson LA, Begueret H, Pineau R, Malrieux C, Dugot-Senant N, Lucchesi C, Chevet E and Delom F: Secretion of protein disulphide isomerase AGR2 confers tumorigenic properties. Elife 5: e13887, 2016.
16. Fessart D, de Barbeyrac C, Boutin I, Grenier T, Richard E, Begueret H, Bernard D, Chevet E, Robert J and Delom F: Extracellular AGR2 triggers lung tumour cell proliferation through repression of p21CIP1. Biochim Biophys Acta Mol Cell Res 1868: 118920, 2021.
17. Maurel M, Obacz J, Avril T, Ding YP, Papadodima O, Treton X, Daniel F, Pilalis E, Hörberg J, Hou W, *et al*: Control of anterior GRadient 2 (AGR2) dimerization links endoplasmic reticulum proteostasis to inflammation. EMBO Mol Med 11: e10120, 2019.
18. Aberger F, Weidinger G, Grunz H and Richter K: Anterior specification of embryonic ectoderm: The role of the Xenopus cement gland-specific gene XAG-2. Mech Dev 72: 115-130, 1998.
19. Zhang JS, Gong A, Cheville JC, Smith DI and Young CYF: AGR2, an androgen-inducible secretory protein overexpressed in prostate cancer. Genes Chromosomes Cancer 43: 249-259, 2005.
20. Thompson DA and Weigel RJ: hAG-2, the human homologue of thexenopus laeviscement gland gene XAG-2, is coexpressed with estrogen receptor in breast cancer cell lines. Biochem Biophys Res Commun 251: 111-116, 1998.
21. Ramachandran V, Arumugam T, Wang H and Logsdon CD: Anterior gradient 2 is expressed and secreted during the development of pancreatic cancer and promotes cancer cell survival. Cancer Res 68: 7811-7818, 2008.
22. Pizzi M, Fassan M, Balistreri M, Galligioni A, Rea F and Rugge M: Anterior gradient 2 overexpression in lung adenocarcinoma. Appl Immunohistochem Mol Morphol 20: 31-36, 2012.
23. Chevet E, Fessart D, Delom F, Mulot A, Vojtesek B, Hrstka R, Murray E, Gray T and Hupp T: Emerging roles for the pro-oncogenic anterior gradient-2 in cancer development. Oncogene 32: 2499-2509, 2013.
24. Salmans ML, Zhao F and Andersen B: The estrogen-regulated anterior gradient 2 (AGR2) protein in breast cancer: A potential drug target and biomarker. Breast Cancer Res 15: 204, 2013.
25. Hrstka R, Nenutil R, Fourtouna A, Maslon MM, Naughton C, Langdon S, Murray E, Larionov A, Petrakova K, Muller P, *et al*: The pro-metastatic protein anterior gradient-2 predicts poor prognosis in tamoxifen-treated breast cancers. Oncogene 29: 4838-4847, 2010.
26. Vanderlaag KE, Hudak S, Bald L, Fayadat-Dilman L, Sathe M, Grein J and Janatpour MJ: Anterior gradient-2 plays a critical role in breast cancer cell growth and survival by modulating cyclin D1, estrogen receptor-alpha and survivin. Breast Cancer Res 12: R32, 2010.
27. Liu D, Rudland PS, Sibson DR, Platt-Higgins A and Barraclough R: Human homologue of cement gland protein, a novel metastasis inducer associated with breast carcinomas. Cancer Res 65: 3796-3805, 2005.
28. Hrstka R, Brychtova V, Fabian P, Vojtesek B and Svoboda M: AGR2 predicts tamoxifen resistance in postmenopausal breast cancer patients. Dis Markers 35: 207-212, 2013.
29. Li Z, Zhu Q, Hu L, Chen H, Wu Z and Li D: Anterior gradient 2 is a binding stabilizer of hypoxia inducible factor-1a that enhances CoCl 2-induced doxorubicin resistance in breast cancer cells. Cancer Sci 106: 1041-1049, 2015.
30. Higa A, Mulot A, Delom F, Bouchecareilh M, Nguyên DT, Boismenu D, Wise MJ and Chevet E: Role of pro-oncogenic protein disulfide isomerase (PDI) family member anterior gradient 2 (AGR2) in the control of endoplasmic reticulum homeostasis. J Biol Chem 286: 44855-44868, 2011.
31. Dimri GP, Lee X, Basile G, Acosta M, Scott G, Roskelley C, Medrano EE, Linskens M, Rubelj I and Pereira-Smith O: A biomarker that identifies senescent human cells in culture and in aging skin in vivo. Proc Natl Acad Sci USA 92: 9363-9367, 1995.
32. Vindeløv LL, Christensen IJ and Nissen NI: A Detergent-trypsin method for the preparation of nuclei for flow cytometric DNA analysis. Cytometry 3: 323-327, 1983.
33. Gillet LC, Navarro P, Tate S, Röst H, Selevsek N, Reiter L, Bonner R and Aebersold R: Targeted data extraction of the MS/MS spectra generated by data-independent acquisition: A new concept for consistent and accurate proteome analysis. Mol Cell Proteomics 11: O111.016717, 2012.
34. Perez-Riverol Y, Csordas A, Bai J, Bernal-Llinares M, Hewapathirana S, Kundu DJ, Inuganti A, Griss J, Mayer G, Eisenacher M, *et al*: The PRIDE database and related tools and resources in 2019: Improving support for quantification data. Nucleic Acids Res 47: D442-D450, 2019.
35. Innes HE, Liu D, Barraclough R, Davies MPA, O'Neill PA, Platt-Higgins A, de Silva Rudland S, Sibson DR and Rudland PS: Significance of the metastasis-inducing protein AGR2 for outcome in hormonally treated breast cancer patients. Br J Cancer 94: 1057-1065, 2006.

36. Tang W, Zhou M, Dorsey TH, Prieto DA, Wang XW, Ruppin E, Veenstra TD and Ambs S: Integrated proteotranscriptomics of breast cancer reveals globally increased protein-mRNA concordance associated with subtypes and survival. Genome Med 10: 94, 2018.

37. Guillon J, Petit C, Moreau M, Toutain B, Henry C, Roché H, Bonichon-Lamichhane N, Salmon JP, Lemonnier J, Campone M, et al: Regulation of senescence escape by TSP1 and CD47 following chemotherapy treatment. Cell Death Dis 10: 199, 2019.

38. Pohler E, Craig AL, Cotton J, Lawrie L, Dillon JF, Ross P, Kernohan N and Hupp TR: The barrett's antigen anterior gradient-2 silences the p53 transcriptional response to DNA damage. Mol Cell Proteomics 3: 534-547, 2004.

39. Hrstka R, Bouchalova P, Michalova E, Matoulkova E, Muller P, Coates PJ and Vojtesek B: AGR2 oncoprotein inhibits p38 MAPK and p53 activation through a DUSP10-mediated regulatory pathway. Mol Oncol 10: 652-662, 2016.

40. Valo I, Raro P, Boissard A, Maarouf A, Jézéquel P, Verriele V, Campone M, Coqueret O and Guette C: OLFM4 expression in ductal carcinoma in situ and in invasive breast cancer cohorts by a SWATH-based proteomic approach. Proteomics 19: e1800446, 2019.

41. Laplante M and Sabatini DM: MTOR signaling in growth control and disease. Cell 149: 274-293, 2012.

42. Yang G, Murashige DS, Humphrey SJ and James DE: A positive feedback loop between akt and mTORC2 via SIN1 phosphorylation. Cell Rep 12: 937-943, 2015.

43. Sarbassov DD, Guertin DA, Ali SM and Sabatini DM: Phosphorylation and regulation of Akt/PKB by the rictor-mTOR complex. Science 307: 1098-1101, 2005.

44. Iannello A, Thompson TW, Ardolino M, Lowe SW and Raulet DH: p53-dependent chemokine production by senescent tumor cells supports NKG2D-dependent tumor elimination by natural killer cells. J Exp Med 210: 2057-2069, 2013.

45. Dahal Lamichane B, Jung SY, Yun J, Kang S, Kim DY, Lamichane S, Kim YJ, Park JH, Jang WB, Ji ST, et al: AGR2 is a target of canonical Wnt/β-catenin signaling and is important for stemness maintenance in colorectal cancer stem cells. Biochem Biophys Res Commun 515: 600-606, 2019.

46. Arumugam T, Deng D, Bover L, Wang H, Logsdon CD and Ramachandran V: New blocking antibodies against novel AGR2-C4.4A pathway reduce growth and metastasis of pancreatic tumors and increase survival in mice. Mol Cancer Ther 14: 941-951, 2015.

47. Armes JE, Davies CM, Wallace S, Taheri T, Perrin LC and Autelitano DJ: AGR2 expression in ovarian tumours: A potential biomarker for endometrioid and mucinous differentiation. Pathology 45: 49-54, 2013.

48. Hu Z, Gu Y, Han B, Zhang J, Li Z, Tian K, Young CYF and Yuan H: Knockdown of AGR2 induces cellular senescence in prostate cancer cells. Carcinogenesis 33: 1178-1186, 2012.

49. Hrstka R, Murray E, Brychtova V, Fabian P, Hupp TR and Vojtesek B: Identification of an AKT-dependent signalling pathway that mediates tamoxifen-dependent induction of the pro-metastatic protein anterior. Cancer Lett 333: 187-193, 2013.

50. Liu Q, Li Y and Yao L: Knockdown of AGR2 induces cell apoptosis and reduces chemotherapy resistance of pancreatic cancer cells with the involvement of ERK/AKT axis. Pancreatology 18: 678-688, 2018.

51. Dong A, Gupta A, Pai RK, Tun M and Lowe AW: The human adenocarcinoma-associated gene, AGR2, induces expression of amphiregulin through hippo pathway co-activator YAP1 activation. J Biol Chem 286: 18301-18310, 2011.

52. Matoulkova E, Sommerova L, Pastorek M, Vojtesek B and Hrstka R: Regulation of AGR2 expression via 3'UTR shortening. Exp Cell Res 356: 40-47, 2017.

53. Tiemann K, Garri C, Lee SB, Malihi PD, Park M, Alvarez RM, Yap LP, Mallick P, Katz JE, Gross ME and Kani K: Loss of ER retention motif of AGR2 can impact mTORC signaling and promote cancer metastasis. Oncogene 38: 3003-3018, 2019.

54. Dumartin L, Alrawashdeh W, Trabulo SM, Radon TP, Steiger K, Feakins RM, di Magliano MP, Heeschen C, Esposito I, Lemoine NR and Crnogorac-Jurcevic T: ER stress protein AGR2 precedes and is involved in the regulation of pancreatic cancer initiation. Oncogene 36: 3094-3103, 2017.

55. Zhao F, Edwards R, Dizon D, Afrasiabi K, Mastroianni JR, Geyfman M, Ouellette AJ, Andersen B and Lipkin SM: Disruption of Paneth and goblet cell homeostasis and increased endoplasmic reticulum stress in Agr2-/-mice. Dev Biol 338: 270-279, 2010.